Journal of Photochemistry & Photobiology, A: Chemistry 442 (2023) 114764

Contents lists available at ScienceDirect

Journal of Photochemistry & Photobiology, A: Chemistry

journal homepage: www.elsevier.com/locate/jphotochem

Construction of novel cyanobacteria-based biological photovoltaic solar cells: Hydrogen and photocurrent generated via both photosynthesis and respiratory system

Buket Bezgin Carbas [a,b,*], Menşure Güler [c], Kamile Yücel [d], Huseyin Bekir Yildiz [c,e,*]

[a] Department of Energy Systems Engineering, Karamanoglu Mehmetbey University, 70100 Karaman, Türkiye
[b] Conductive Polymers and Energy Applications Laboratory, Karamanoglu Mehmetbey University, 70100 Karaman, Türkiye
[c] Department of Metallurgical and Materials Engineering, KTO Karatay University, 42020 Konya, Türkiye
[d] Department of Medical Biochemistry, Faculty of Medicine, KTO, Karatay University, Karatay, 42020 Konya, Türkiye
[e] Department of Mechanical Engineering, Bartin University, 74100 Bartin, Türkiye

ARTICLE INFO

Keywords:
Conjugated polymer
Biological photovoltaic solar cell
Cyanobacteria
Hydrogen generation
Photosynthesis
Respiratory system
Photocurrent

ABSTRACT

Biological photovoltaic (BPV) cells use biological organisms in order to produce clean electrical power by capturing solar energy. In this study, a cyanobacteria based BPV cell was constructed and it generated H_2 gas and photocurrent via photosynthesis and respiratory system. This kind of BPV cell was constructed in which the cathode and photoanode are gold electrodes coated with different conjugated polymers and these polymers are combined to Pt or Au nanoparticles with oligoaniline bonds. Unlike the cathode electrode, a kind of cyanobacteria (Leptolyngbia sp.) was used in the design of photoanode and bounded to Au NPs with oligoaniline bonds. For the configuration of cathode in BPV cell, a gold electrode was first coated with a dithienylpyrrole-based conductive polymer with an amine open-ended aniline functional group. This conductive polymer was then attached to mercapto-aniline functionalized Pt nanoparticles with oligoaniline bonds. In the case of photoanode in BPV cell, this time, a dithienopyrrole-based conductive polymer with an aniline subunit was coated on another Au electrode surface via electrochemical polymerization. This polymer provides to connect oligoaniline modified Au nanoparticles with coating cyanobacteria. Some control and optimization experiments for photoanode of the system were done in order to understand photosynthesis formation and get efficient photocurrent from BPV cell. The system was illuminated under visible light and a constant potential and then the decomposition of water in BPV solar cell system was observed via photosynthesis by cyanobacteria with the formation of H_2 and O_2 gases besides photocurrent generation. Another photocurrent generation via respiratory system of cyanaobacteria was also investigated in the medium of glucose after diuron (PS II inhibitor an inhibitor) was added into medium. By using two different properties (photosynthesis and respiratory system) of cyanobacteria, BPV solar system generates high amount of photocurrent and hydrogen.

1. Introduction

Today, many countries are increasing their efforts to use new, clean and sustainable energy sources as an alternative to fossil fuels. Renewable energy sources are very crucial for global future plans of people [1–4]. Unlike fossil fuels, which are dwindling and becoming less sustainable, scientist tries to find clean and economic energy sources [5]. Related studies suggest that solar power is the most important renewable energy source and solar typed all energy conversion systems are more efficient and sustainable than other options [6]. Photovoltaic solar cells, plants, cyanobacteria and green algae harness the energy from the sun to produce electricity. Solar cells and other photosynthesis-based organisms produce energy in different ways. Photoelectrochemical cells are solar cells that use the energy from the sun to produce electricity or hydrogen [7–9]. In biological photovoltaic solar cell (BPV), water hydrolyzes with the help of photosynthesis and it is water that provides electrons to the system. Photosynthetic microorganisms active in the BPV cell continue their vital development, so they have a sustainable habitat. They store metabolites in their cells and thus they can also be grown by inexpensive methods and tend to generate energy even

* Corresponding authors at: Department of Energy Systems Engineering, Karamanoglu Mehmetbey University, 70100 Karaman, Türkiye.
E-mail addresses: bcarbas@kmu.edu.tr (B.B. Carbas), huseyinbekir.yildiz@karatay.edu.tr (H.B. Yildiz).

https://doi.org/10.1016/j.jphotochem.2023.114764
Received 13 February 2023; Received in revised form 5 April 2023; Accepted 11 April 2023
Available online 15 April 2023

under dark conditions. These characteristics make it superior for a typical photovoltaic cell [10]. Significant efforts have been made in the development of BPVs in recent years to meet the energy needs from solar energy in the future. With the biological energy production cycle, an average of 30 μA photocurrent was obtained by arresting Os complex-modified conductive polymers, hydrogels, combined multi-surface structures, p-added silicon structures, Pt nanoparticles cross-linked with bis aniline [11–16]. There are also studies of BPV obtained by binding to Os-redox polymer, 3D graphene and cytochrome-c typed conductive polymer electrode [17–21]. Moreover, the effect of these conductive structures on electron transfer was also investigated. The studies showed that an average of 40 μA photocurrent was produced. In addition, Hasan et al. investigated the mediator effect of water-soluble quinone derivatives and obtained photocurrent by arresting the TM on a bare Au electrode [22]. Green algae, another photosynthetic material, have also been used to make BPVs. In a BPV study conducted by Hasan et al., photocurrent generation studies were carried out using Paulschulzia pseudovolvox [19]. Fong Lee et al. created a typical anode electrode for the BPV system by means of shielding using an indium tin oxide coated glass surface with graphene, and then added the photosynthetic Chlorella sp. to the BPV to generate a biofilm on the anode platform. With this study, it was observed that nanomaterials increased electron transfer when light was sent to the system. As a result of studies, it has been shown that algae come into contact with nano sized structures and these structures interact with the membrane located outside the algae cell [23]. MacCormick et al., on the other hand, formed biofilms by coating Dunaliella tertiolecta and Chlorella vulgaris algae on ITP surface under controlled conditions. Thanks to these biofilms formed in BPV, a neighbor communication among the algae and anode was established and it resulted in high photocurrents. This high photocurrent value continued to be stable up to 30 days [24]. Amidst the photosynthetic organisms, cyanobacteria are the most favored for power generation from sunlight in BPVs by the reason of their high efficiency besides the possibility of direct energy production and the convenience of environmental compatibility [25]. Recently, a large number of cyanobacteria-based BPV studies have been conducted. Geobacter sulfurreducens [26], synechococcus sp. PPC 7942, anabaena variabilis [25], synechocystis sp. PCC 6803 [27,28], shewanella oneidensis [29] coated graphite, carbon brush, Pt, Au and indium tin oxide glassy electrodes [1] can be given as examples of BPV studies that generate photocurrent by providing fast electron transfer. In the studies researched by our group, photocurrents were produced with the help of fast electron transfer, which is carried out by connecting lyptolyngbia sp type cyanobacteria on Os complex modified polymers and conductive polymer/Au nanoparticles type structures [30,31]. In addition, Howe and his work group were able to generate electricity in both light and dark environments without using a mediator in the BPVs and they made this by creating cyanobacteria-based biofilms [8]. Reports have shown that the stable presence of cyanobacteria in BPV cells for long periods makes the power generation facility even more effective.

Today, hydrogen can be obtained from fossil fuels, natural gas conversion, conversion of biologically sourced liquids, coal and biomass gasification, thermochemical and nuclear production, electrolysis of water or photoelectrochemical separation of water [32–38]. However, these technologies are either too expensive or not environmentally friendly. While 5% of the hydrogen production is provided primarily by the electrolysis of water, 95% is provided from fossil fuels. Hydrogen production studies have gained momentum as a result of photoelectrochemical separation of water using various catalysts or conductive structures in solar cells. The photocurrent and hydrogen production have been successfully carried out by photoelectrochemical decomposition of water in solar cells created by using various conductive structures and photosensitive dyes by our study group [39,40]. Although there are various chemical methods and techniques by which hydrogen can be produced, as described above, hydrogen production by microbial biotechnologies attracts a lot of attention, especially because they are renewable and relatively inexpensive in terms of sustainability. Under anaerobic conditions, microbial cells can produce hydrogen by fermenting carbohydrate-rich suspension liquids, including industrial and domestic wastewater. Alternatively, photosynthetic microbial cells allow photobiological hydrogen production. By using microbial cells capable of photosynthesis with oxygen, hydrogen can be produced with the help of abundant and sustainable resources such as water and sun and without the need for organic matter supplementation. However, today, there are very few BPV studies that produce H_2 gas on the cathode side by using photosynthetic biomaterials such as cyanobacteria on the anode side. The reason for this is that, as Rozendal et al. mentioned in their study, the desire of oxygen and protons, which are formed as a consequence of oxidation of water by photosynthesis, to reconvert to water in terms of energy is higher than the desire of protons to be reduced to H_2 gas and therefore, the cathode side must be completely free of oxygen in order for H_2 gas to form at the cathode [41]. Sustainable H_2 gas production was achieved by using photosynthetic microbial cells by separating the anode and cathode by placing proton-conducting or permeable membranes such as cationic ion exchange membrane or Nafion, and purifying the cathode from oxygen [27,42–44]. In recent studies, it has been shown that BPVs made using photosynthetic microorganisms can produce both photocurrent and hydrogen. Howe and the working group made synechocystis sp. and obtained photocurrent in both dark and light environments by adding $[FeCN_6]^{-4/-3}$ electron mediator to the environment in cyanobacteria-based BPVs. Protons produced as a result of photosynthesis in the light environment also provided hydrogen production in the dark environment by giving a 1–1.4 V bias potential [45]. Schumann et al., in their study, in synechocystis sp cyanobacteria-based PBV, both photocurrent and hydrogen production as a result of photosynthesis, and PS II inhibitor 3-(3,4-dichlorophenyl)-1,1-dimethylurea (DCMU) were put into the environment and the cyanobacteria were actively involved in the respiratory system. They obtained photocurrent and hydrogen production with protons and electrons from PS I. They also observed that hydrogen and photocurrent increased when glucose was added to the cell from the outside, since the respiratory system initially oxidized carbonaceous substances. During hydrogen production, 0.65 V bias potential was given to the system in both environments [46].

In the light of these information, BPV that can produce photocurrent and hydrogen at the same time by using both photosynthesis and respiration properties of cyanobacteria under constant potential and visible region light will be made by using Leptolyngbia sp. cyanobacteria. A photoanode will be formed by coating cyanobacteria on the structure that will be formed as a result of connecting aniline-modified gold nanoparticles (Au NP) to the coated gold electrode with conductive oligopyrrole bonds by electrochemical polymerization with aniline-functionalized DTP conductive polymer (P(DTP-Ph-NH_2)). The structure formed electrochemically with aniline-functionalized Pt NPs with aniline-functional SNS conductive polymer (P(SNS-Ph-NH_2)) on a modified gold electrode with oligoaniline bonds will act as cathode. When the system is operated under a fixed potential by illuminating the visible region with light, water will decompose by oxidation through photosynthesis by cyanobacteria, and photocurrent will occur with the transport of electrons released by the oxidation of water to the anode, and hydrogen gas will be produced by the reduction of protons on the cathode side by Pt NPs. Then, when the PS II inhibitors called diuron and 3-(3,4-dichlorophenyl)-1,1-dimethylurea (DCMU) are put into the medium and the cell is illuminated under constant potential in the glucose environment, the electrons to be formed in PS I by oxidation of glucose are transferred to the anode. Photocurrent and hydrogen gas will occur simultaneously with the transport and reduction of protons to the cathode. Thus, a high rate of hydrogen and photocurrent will be obtained by taking advantage of both photosynthesis and respiration of cyanobacteria.

Nowadays, BPV studies have become quite popular. In recent studies, it has been shown that BPVs made using photosynthetic microorganisms

can produce both photocurrent and hydrogen. The majority of BPV studies to produce electricity and/or hydrogen today are with the help of photosynthesis. In this study, BPV generates photocurrent and hydrogen production by using the respiration feature of cyanobacteria together with photosynthesis. The production of electricity and hydrogen by using the respiration feature of BPVs and photosynthetic biological materials related studies is almost non-existent in the relevant literature. With this study, even in conditions where photosynthesis is difficult, electricity and hydrogen production will be possible by taking advantage of the respiration feature of cyanobacteria.

2. Experimental section

2.1. Materials

4-(2,5-di(thiophen-2-yl)-1H-pyrrol-1-yl)benzamine (SNS-Ph-NH_2) monomer and 4-(4H-dithieno[3,2-b:2′,3′-d]pyrrol-4-yl)aniline (DTP-Ph-NH_2) were reported as in the literature [47,48] and details were given in supplementary. Among the photosynthetic microorganisms, cyanobacteria (Leptolyngbia sp.) were purchased from Carolina™ (USA). The cyanobacteria (Leptolyngbia sp.) to be used in this study were reproduced according to the literature [11]. In summary, propagation was carried out at room temperature, in a low ion intensity environment and under a white fluorescence lamp with a photon power of 40 μmol, adjusted to 12:12 light/dark. Cells were then incubated at 20 °C for 10 min. It was centrifuged at 4000 rpm, washed with electrolyte and centrifuged again under the same conditions. The obtained Leptolyngbia sp. cells were resuspended with the same electrolyte as 1 g/ml solution and immediately used for photoelectrochemical measurements. The remaining materials were used in the experiments as they were obtained from the Sigma Aldrich Company.

2.2. Methods

The details related with reproduction of cyanobacteria, synthesis of monomers (dithienyl pyrrole (SNS) and dithienopyrrole (DTP) derivatives) and their polymerization processes are given in supplementary information. BPV cell was constructed with a photoanode and cathode electrodes containing conductive polymer-coated gold or Pt nanoparticles (Pt NPs). Firstly, cathode electrode construction was done. An Au electrode was electropolymerized with SNS-Ph-NH_2. After that, Pt NPs were bound to P(SNS-Ph-NH_2) polymer film with oligoaniline bonds

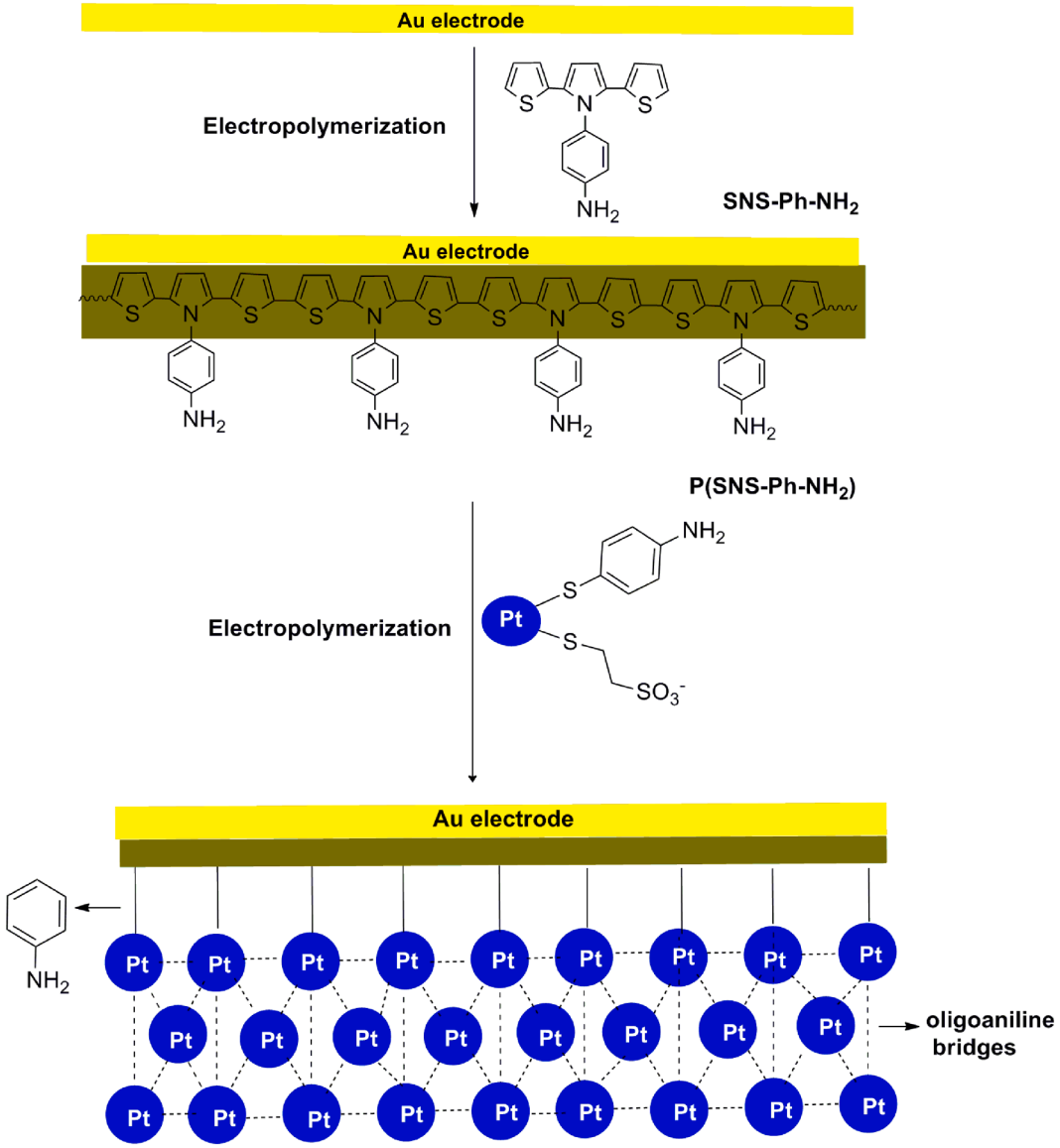

Scheme 1. Schematically representation of cathode electrode construction.

from its –NH_2 end. DTP-Ph-NH_2 monomer was also electropolymerized on another Au electrode in order to construct the photoanode part of BPV cell. Au NPs were synthesized with aniline ends in order to get a connection between P(DTP-Ph-NH_2) and Au NPs with oligoaniline bonds. After that cyanobacteria was matured on this electrode system, some optimization and control experiments (the amount of cyanobacteria, thickness of the electrode and cycle number polymerization on the electrode) were studied to get maximum photocurrent value.

2.2.1. Construction of cathode electrode of BPV

Scheme 1 represents the formation of cathode electrode in BPV. First of all, SNS-Ph-NH_2 was synthesized electrochemically as given in Scheme-SI-1. Monomer was electropolymerized on Au electrode, as seen in repetitive cyclic voltammogram (Figure SI-1). Pt NPs will be functionalized with mercaptoaniline. These two structures will be bounded with oligoaniline groups.

2.2.1.1. Preparation of Pt NPs functioned with mercaptoaniline. Three different mixture solutions were prepared in order to synthesize of these nano-sized materials. The first solution was formed by dissolving of $PtCl_4$ (300 mg) in hexylamine (75 mL). The second one had a mixture of dissolving thioaniline (35 mg) and the sodium salt (180 mg), 2-mercaptoethanesulfonic acid ($1.1x10^{-3}$ mol) in a methanol/hexylamine (30 mL) solution (1:1 by volume). Solution number three was prepared by mixing sodium borohydride (300 mg) into to a water/methanol mixture (1:1 by volume) (40 mL). After adding solution number three to solution number one at room temperature with vigorous stirring, the color of the solution changed to brown color in seconds and solution number two was added to this brown solution after 1 min. Three minutes later, distilled water (200 mL) was put into the solution and mixed for 15 min. The solution was put into the separatory funnel and the water phase of the mixture was removed. The organic part was rewashed repeatedly with water. For next step, sodium salt of 35 mg, $2.8x10^{-4}$ mol of thioaniline and 180 mg of $1.1x10^{-3}$ mol of mercaptoethane sulfonic acid dissolved in ethanol solvent (15 mL) was put into the organic part. The obtaining solution was mixed during the night. The black part of the mixture was collected after being centrifuged several times and washed repeatedly with the solvent of diethyl ether. It was understood that the prepared Pt NPs were 4–5 nm in diameter. These NPs were characterized by SEM analysis (Figure SI-2).

2.2.1.2. Design of a cathode (P(SNS-Ph-NH_2)/Pt NP) electrode (P(SNS-Ph-NH_2)/Pt NP) in BPV. SNS-Ph-NH_2 monomer was electropolymerized on the Au electrode surface in the medium of 0.1 M $NaClO_4$/0.1 M $LiClO_4$/acetonitrile solution via cyclic voltammetry. Afterwards, Pt NPs functionalized with mercaptoaniline were polymerized by electropolymerization method in phosphate pH = 7.4 phosphate buffer medium via cyclic voltammetry. Thus, it was bonded to P(SNS-Ph-NH_2) polymer which was polymerized by electropolymerization method on the Au electrode. The redox pair seen around 0.1 V on the cyclic voltammogram indicates the formation of bis aniline cross-links (Figure SI-3).

2.2.2. Construction of photoanode electrode of BPV

For design of photoanode electrode in BPV, DTP-Ph-NH_2 was firstly synthesized with a synthesis procedure in Scheme SI-2. Moreover, DTP-Ph-NH_2 was also electropolymerized and its electropolymerization details were given in Figure SI-4.

2.2.2.1. Synthesis of aniline-functionalized Au NPs. Au NPs functionalized with 2-mercaptoethane sulfonic acid and p-aminothiophenol were added with 10 mL of ethanol solution containing 197 mg of $HAuCl_4$ and 5 mL of methanol solution containing 42 mg of mercaptoethane sulfonate and 8 mg of p-aminothiophenol into 2.5 mL of glacial acetic acid, and this new solution was dissolved in 2.5 mL of glacial acetic acid. It was prepared by mixing in an ice bath for 1 h [49]. Then, 1 M 7.5 mL of $NaBH_4$ solution was added dropwise to this solution until a black solution was obtained. The new black solution was stirred in the ice bath for another 1 h, then removed from the ice bath and stirred at room temperature for another 14 h. The resulting nanoparticles were washed twice with methanol, ethanol and diethyl ether solutions and then centrifuged. These Au NPs were characterized by transmission electron microscopy. When examined by transmission electron microscopy (TEM), the dimensions of the particles were estimated to be 8.5 nm. The photograph of the particles taken with the help of TEM is as in Figure SI-5 [49].

Electropolymerization with DTP-Ph-NH_2 homopolymer and aniline-modified AuNP in 0.1 M phosphate buffer solution (pH = 7.4) with the aid of CV between the potentials of −0.1 V and + 1.1 V at a scan rate of 100 mV/s are linked to each other by oligoaniline bonds. In this electropolymerization experiment, graphite electrode (d = 5 mm) and Ag/AgCl electrode were utilized as auxiliary and as reference electrode, respectively.

2.2.2.2. The design of the photoanode electrode. The gold electrodes were washed with ultrapure water and dried at room temperature. The (DTP-Ph-NH_2) monomer (5 mg/mL) synthesized under the above-mentioned conditions was then on the gold electrode surface in 0.1 M $TBAPF_6$/dichloromethane/acetonitrile medium via cyclic voltammetry with a scan rate of 100 mV/s between −0.1 V and + 1.2 V. It was electrochemically polymerized. Aniline-modified 100 mM AuNP solution was added into 0.1 M phosphate buffer solution (pH = 7.4) and electropolymerization technique was used on the gold electrode via cyclic voltammetry with a scan rate of 100 mV / s between the potentials of 0.1 V and + 1.1 V. P(DTP-Ph-NH_2) is attached to the film by oligoaniline bonds. In this electropolymerization experiment, the platinum wire was used as the counter electrode and the Ag/AgCl electrode as the reference electrode. Then, cyanobacteria matured in a special culture medium were coated on the modified Au electrode with the optimum amount of P (DTP-Ph-NH)/Au NPs structure. Then, the dialysis membrane immersed in phosphate buffer (pH 7.4) was placed on the cyanobacteria to prevent the cyanobacteria from falling off the surface of the electrode and firmly attached to the surface of the electrode with the help of a rubber and money film. Thus the photoanode of BPV was completed (Scheme 2).

2.2.3. Photocurrent and hydrogen generation studies in BPV

H-type cells were used in photocurrent experiments Au electrode modified with conductive polymer (P(DTP-Ph-NH_2)/Au NPs/cyanobacteria) to be used as anode in BPV cell and Au electrode covered with P(SNS-Ph-NH_2)/Pt NPs 50 mm away from it to serve as bio-cathode in photovoltaic cell. They will be in tube sections facing each other, with a distance of 50 mm and they will be separated from each other by a proton-permeable membrane (Nafion membrane). A multimeter will be placed across the resistor. A solar simulator with a custom-made photochemical system was used for photocurrent measurements. This photochemical system consists of an Oriel brand 300 W Xe lamp (Oriel Model 6258), an Oriel brand 2 nm resolution monochromator (Oriel Model 74000) and an Oriel brand chopper (model 76994). The process of converting the data to digital data was done by a phase sensitive detector (Stanford Research Model SR 830 DSP). The current cut-off frequency was performed via a Stanford Research brand pulse-retardant generator. For the constant potential experiments carried out in the study, a potentiostat/galvanostat (EG&G Model 263) was used besides the electrodes mentioned above.

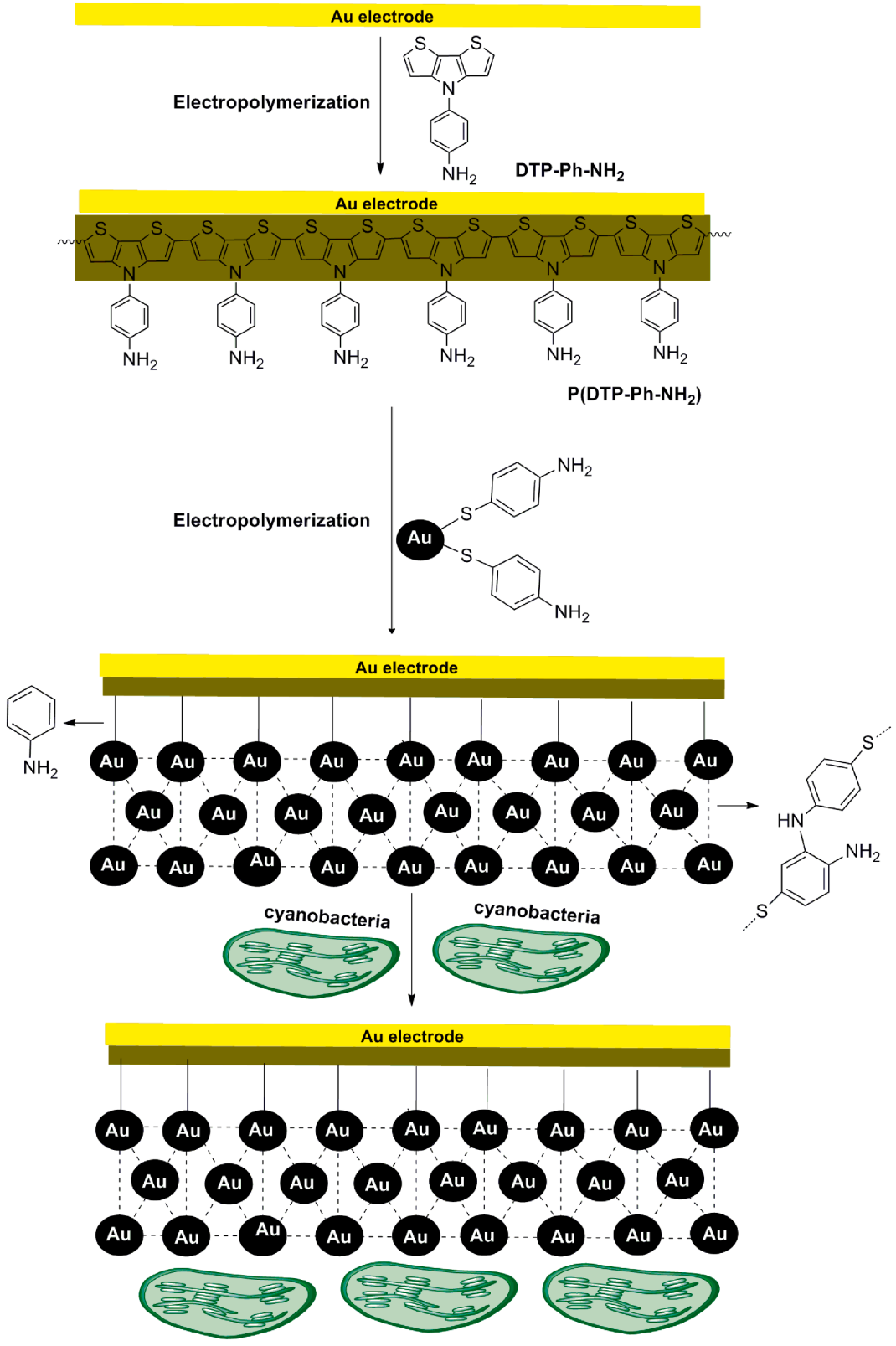

Scheme 2. Schematically representation of photoanode electrode construction.

3. Results and discussion

3.1. The optimization studies for cathode (P(SNS-Ph-NH_2)/Pt NPs) electrode of BPV cell

One of the most important properties of Pt NPs is hydrogen peroxide reduction to water via electrocatalyzing. In the real purpose of the project, Pt NPs will reduce the protons come out of the oxidation of water to H_2 gas. It is thought that the surface optimizations required for the fastest electron transfer from the electrode to the Pt NP will be found by using the reduction of hydrogen peroxide and the optimum conditions that will emerge from this will be the same for the transfer of protons to H_2 gas during the separation of water [50] (Figure SI-7). The P(SNS-Ph-NH_2)/Pt NPs cathode electrode is firstly optimized with the cycle number via cyclic voltammetry in order to find best coupling bounding to Pt NPs on a Au electrode (1 cm^2 area) with oligoaniline bonds. In this optimization study Pt NPs were bonded by electropolymerization on the conductive film polymerized with 100 cycles, while the concentration of Pt NPs was kept constant at 1 mg/mL. Experiments were achieved in phosphate buffer (pH = 7.4) medium. For optimization study, Pt NPs were bonded to the electrode covered with oligoaniline composite bonds of polymer by electropolymerization at different number of cycles (40, 60, 80 and 100 cycle numbers in the medium of hydrogen peroxide (9 mM) in between 0.2 V and 0.6 V). As a result of the current differences obtained in the voltammogram as a result of hydrogen peroxide reduction to water by Pt NPs, the best number of cycles in order to bind Pt NPs to the conjugated polymer was obtained. As the number of electropolymerization cycles increased to form the composite, it was observed that the current difference increased in the voltammograms taken. In this case, it continued until the number of 80 cycles, and the current difference decrease was observed in the 100th cycle. The reason for the increase in the current difference up to 80 cycles can be considered as the increase in the amount of Pt NPs bound by the oligoaniline composite bonds in the composite.

In this experiment, which was repeated three times and data were obtained close to each other as a result of all three experiments, it was decided that 80 cycles would be the optimum cycle number to bind Pt NPs to P(SNS-Ph-NH_2) polymer with composite oligoaniline bonds. In all of these optimization studies, after SNS-Ph-NH_2 monomer was polymerized on the Au electrode with an area of 1 cm^2 using 80 cycles, Pt NPs were bonded to P(SNS-Ph-NH_2) polymer by electropolymerization (Figure SI-8).

Another optimization study is to obtain the number of cycles in the electropolymerization of the monomer. In experiments of the first optimization studies, the SNS-Ph-NH_2 monomer was polymerized by using 80 cycles. In this optimization study, 10, 40, 60, 80, 100 and 120 cycles of SNS-Ph-NH_2 monomer were polymerized on the Au electrode by electropolymerization. P(SNS-Ph-NH_2)/Pt NPs modified Au electrode to be used as cathode in the project was obtained by applying Pt NPs (1 mg/mL) on the polymer films obtained through these various cycle numbers, by applying 80 cycles in CV, to the polymer via electropolymerization. Cycles were taken in a potential difference range between 0.2 to −0.6 V using 9 mM hydrogen peroxide in a phosphate buffer medium (pH = 7.4). The highest current difference in the cyclic voltammograms was obtained for 100th cycle of P(SNS-Ph-NH_2) polymer. When the 120-cycle polymer electrode was used, the current difference in the voltammogram decreased. At 120 cycles, however, the thick polymer film was obtained and not enough electrons to reach the electrode (Figure SI-9). SEM images of P(SNS-Ph-NH_2) and P(SNS-Ph-NH_2)/Pt NPs modified gold electrodes were given in Figure SI-10.

3.2. The control and optimization studies for photoanode (P(DTP-Ph-NH_2)/Au NPs /cyanobacteria) electrode of BPV cell

3.2.1. The control experiments for P(DTP-Ph-NH_2)/Au NPs/cyanobacteria electrode

The control experiments were done repeatedly in order to understand how the current is generated by the gold electrode modified with the P(DTP-Ph-NH_2)/Au NPs/cyanobacteria electrode. First, when the gold electrode modified with this structure was dipped in pure ethanol solvent and 1 solar unit was sent onto it, no photocurrent formation was achieved. This showed us that the cell is only responsive to water and that the current was obtained by electron transfer during the formation by the water oxidation as a result of photosynthesis. In addition, instead of the structure formed on the gold electrode, only the cyanobacteria was immobilized and the phosphate buffer (pH = 7.4) of the cyanobacteria-coated gold electrode was immersed in solution (water) and the visible region light of 1400 W/m^2 was sent, and the system did not form. In the third photocurrent control experiment, a photocurrent of 366nA was observed when the 500 mg/mL cyanobacteria-coated gold electrode was immersed in a phosphate buffer (pH = 7.4) involving phenyl-p-benzoquinone solution (0.410 μmol) and a visible light of 1 solar unit was sent to the system (Fig. 1**(a)**). This suggests that a structure that accelerates electron transfer is needed for the transfer of electrons, which is obtained by the water oxidation as a result of photosynthesis to the electrode. In another control experiment, using the gold electrode electropolymerization technique, after being covered with polymer film (40 cycled), 500 mg/mL cyanobacteria was coated on electrode covered with polymeric film. P(DTP-Ph-NH_2)/cyanobacteria structure on gold electrode was dipped into the buffer solution and the system was constructed. When visible light of 1400 W/m^2 power was sent, the amount of photocurrent obtained under 0 V constant potential increased to 2.18μA (Fig. 1**(b)**). This event showed how effective the conductivity of the polymer was in the transfer of electrons to the electrode resulting from photosynthesis. In the last control experiment, after the P(DTP-Ph-NH_2) polymer was electropolymerized on the gold electrode using 40 cycles, 100 mM Au NP solution functionalized with aniline was attached to the conjugated polymer film with oligoaniline chains using 40 electropolymerization cycles. When the gold electrode modified with P(DTP-Ph-NH_2)/Au NP/cyanobacteria was dipped into the buffer solution. The amount of photocurrent obtained under 0 V constant potential increased up to 6.93μA (Fig. 1 **(c)**). 500 mg/mL cyanobacteriawas used to coat for the fabrication of P(DTP-Ph-NH_2)/Au NPs/cyanobacteria structure was coated as in Au electrode/cyanobacteria and P(DTP-Ph-NH_2)/cyanobacteria electrodes.

3.2.2. The cycle number optimization experiments for P(DTP-Ph-NH_2)/Au NP/cyanobacteria electrode

One of the characterization studies of P(DTP-Ph-NH_2)/Au NPs/cyanobacteria on gold electrode structure is the cycle number optimization study in cyclic voltammetry to bind Au NPs to the conjugated polymer film. In this study, polymer prepared using 40 polymerization cycles was coated on the gold electrode on the film, and then aniline-functionalized (100 mM) Au NPs solution was used using 20, 30, 40, 50, 60, 70 and 80 electropolymerization cycles, and conductive polymer with oligoaniline bonds attached to the film. After attaching 500 mg/mL cyanobacteria on these structures, when P(DTP-Ph-NH_2)/Au NPs/cyanobacteria structure was dipped into the buffer solution and 1400 W/m^2 visible region light was sent to the system, various amounts of photocurrents were obtained (under 0 V constant potential). High amount of photocurrent was obtained as the number of cycles increased to cover Au NPs on the polymer film. This situation continued until the number of 60 cycles. The reason for this can be considered as the increase in the amount of Au NPs and the fastest electron transfer as a result. On the other hand, although the amount of Au NPs increased as a result of the applied 70 and 80 cycles, the reason for the photocurrent increase to reach saturation can be shown as the rapidly increasing confusion in the conduction paths with

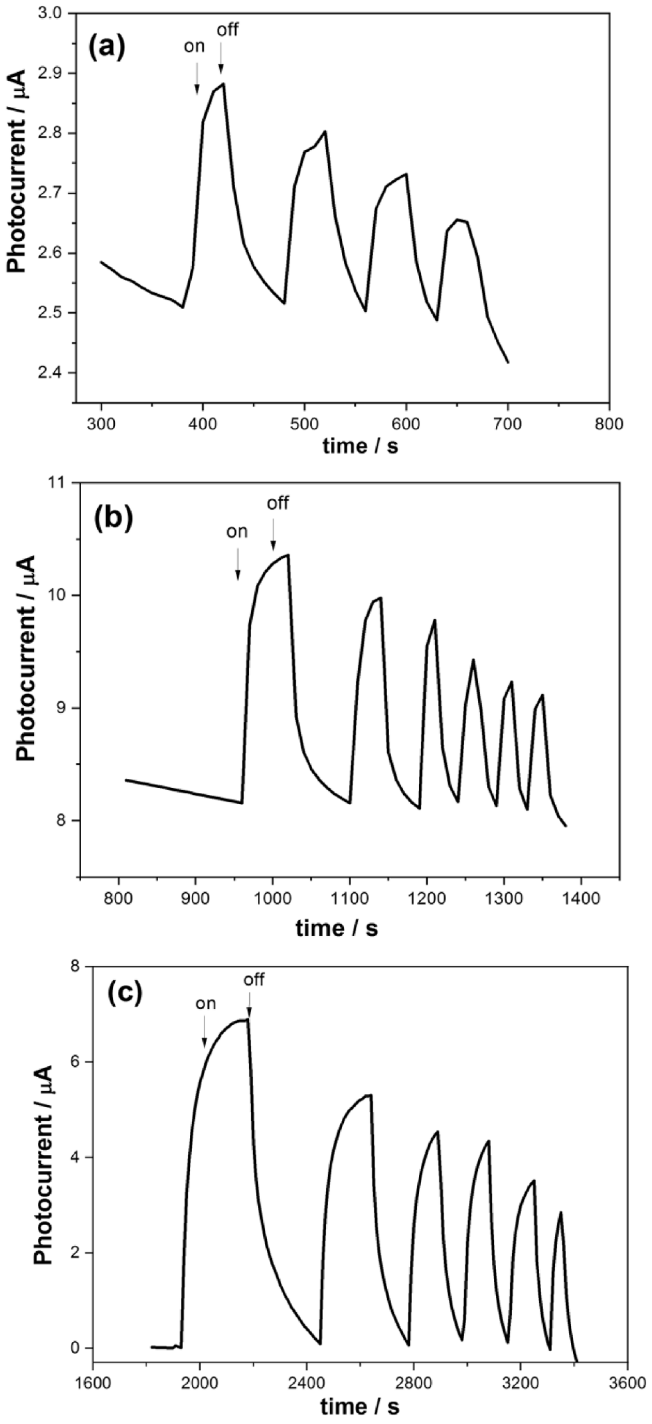

Fig. 1. Demonstration of the photocurrent produced by the oxidation of water as a result of photosynthesis, by chronoamperometric on–off study (a) 0.410 μmol phenyl-p-benzoquinone coated with cyanobacteria on Au electrode (b) Au electrode modified with the P(DTP-Ph-NH_2)/cyanobacteria structure and (c) gold electrode modified with P(DTP-Ph-NH_2)/Au NPs/Cyanobacteria structure under visible light.

the increase in the number of Au NPs, resulting in a decrease for conductivity and the speed of electron transfer. In this experiment, 60 cycles was chosen as the optimum cycle number to bind Au NPs on the polymer film (Fig. 2).

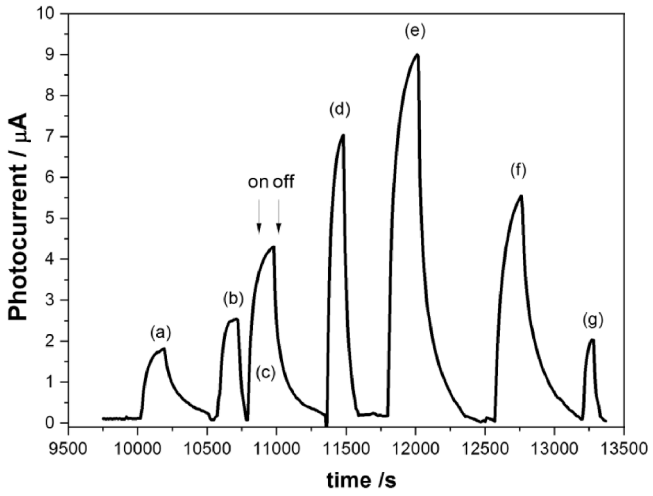

Fig. 2. Chronoamperometric on–off of the photocurrents generated by the electrode modified with the P(DTP-Ph-NH_2)/Au NPs/cyanobacteria (bounded at different cycle numbers (a) 20, (b) 30, (c) 40, (d) 50, (e) 60, (f) 70, (g) 80) structure in order to to bind AuNP on polymer film polymerized electrochemically after 40 cyles of DTP-Ph-NH_2 monomer. 500 mg/mL cyanobacteria were used for coating on each P(DTP-Ph-NH_2)/Au NPs structures.

3.2.3. The amount optimization experiments of cyanobacteria for P(DTP-Ph-NH_2)/Au NPs/cyanobacteria electrode

Another of the characterization studies of P(DTP-Ph-NH_2)/Au NPs/cyanobacteria structure is the best amount of the cyanobacteria that cause photosynthesis. In all photochemistry characterization studies carried out so far, 500 mg/mL cyanobacteria P(DTP-Ph-NH_2)/Au NPs was used by immobilizing it on a modified gold electrode and current measurements were studied. In the optimization study, the polymer prepared with 40 electropolymerization cycles was attached to the aniline-functionalized (100 mM) Au NPs solution on the film with oligoaniline bonds using 60 electropolymerization cycled. Then, 250, 500, 750 and 1000 mg/mL cyanobacteria using P(DTP-Ph-NH_2)/Au NPs was immobilized on the electrode. Phosphate buffer photocurrent measurements were studied in the system (under 0 V constant potential and the visible region light of 1400 W/ m^2 power). It has been observed that the photocurrent increases up to a concentration of 750 mg/mL. The studies observed that the photocurrent values obtained from the electrodes prepared using a concentration of more than 750 mg/mL decreased. The reason for this could be explained as increasing cyanobacteria concentration, thickening of the biocomponent surface and preventing the electrons transfer to the electrode, which is formed by water oxidation as a result of photosynthesis. Therefore, 750 mg/mL, the optimum concentration amount for cyanobacteria was chosen.

3.2.4. The thickness optimization experiments for P(DTP-Ph-NH_2)/Au NPs/cyanobacteria electrode

Another optimization study for the characterization of P(DTP-Ph-NH_2)/Au NPs/cyanobacteria structure is to find the optimum thickness of the polymer film coated on the gold electrode. In all experiments of the previous optimization run, the DTP-Ph-NH_2 monomer was polymerized with 40 cycles. In this optimization study, 20, 40, 60, 80 and 100 cycles of DTP-Ph-NH_2 monomer were polymerized on the gold electrode by electropolymerization. Aniline-functionalized (100 mM) Au NPs solution on the polymer films obtained by these various cycle numbers was bonded to the conjugated polymer film with oligoaniline chains using 60 electropolymerization cycles. Then, 750 mg/mL cyanobacteria was coated on the P(DTP-Ph-NH_2)/Au NP electrode and a modified gold electrode with P(DTP-Ph-NH_2)/Au NPs/cyanobacteria structure as the photoanode was obtained. It was produced by immersing this electrode in phosphate buffer (pH = 7.4) and oxidizing water as a result of photosynthesis under visible light at 1400 W/m^2

power. It was observed that the highest value in the produced photocurrents was with 60-cycled P(DTP-Ph-NH_2) polymer. The photocurrent value decreased when 80 and 100 cycled polymer electrodes were used. 60 cycled polymer film is the best values of thickness and conductivity in order to transfer electrons. In cycles of more than 60 cycles, the film was very thick in order to transfer of electrons formed by the water oxidation as a result of photosynthesis and it was explained as not reaching the electrode enough (Fig. 3).

3.3. Photocurrent and hydrogen generation studies in BPV cell

3.3.1. O_2 gas generation in BPV cell

The chronoamperometric on–off study performed after determining the optimum conditions for the produced BPV is another characterization study of the modified gold electrode with P(DTP-Ph-NH_2)/AuNPs /cyanobacteria structure. The BPV was illuminated for a while at a constant potential of 0 V with a fixed light source (1400 W/m^2) and then the lighting was terminated. This process was repeatedly tested. The current decreased after the process was repeated each time. The reason for this photocurrent decrease is explained as the penetration of the O_2 gas formation was obtained by the water oxidation into the forward electron transfer rate that creates the current. Different experiment has been done as a proof of this statement. Here, the removement of the O_2 gas formation was focused on by adding the bilirubin oxidase enzyme (1.5 mg/mL) to the electrolyte, that is, to the buffer solution and then to operate the BPV at a constant potential of 0 V by illuminating it [39,40]. When the bilirubin oxidase enzyme was added to the medium and the electrode was illuminated with a 1400 W/m^2 light source for some time and the light source was turned off (on–off), no decrease was observed in the amount of photocurrent obtained. In this case, the photocurrent drop supported the reason we explained (Fig. 4).

Clark type electrode system was utilized to understand the amount of oxygen is obtained in the water when the BPV is illuminated for a time. Fig. 5 shows obtained currents by illuminating the visible region under BPV 1400 w/m^2 power for 2.5, 5, 10, 15, 20 and 25 min. After the system was illuminated for 25 min, the amount of oxygen generation by the water oxidation as a result of photosynthesis by the gold electrode modified with P(DTP-Ph-NH_2)/Au NPs/Cyanobacteria structure was calculated as 6.3 x10^{-9} mol/cm^2 (Fig. 5).

3.3.2. Power generation of BPV cell

The electricity production of the BPV was determined by the polarization curve with series connected resistors (ranging from 100 Ω to 10 kΩ) with the BPV during measurements made under visible light illumination. The increase in power outputs is calculated from 17 to 41.5 mW/m^2 in the light environment. The maximum power generation of the BPV at pseudo steady state is reached at 46.50 mW/m^2 at a current density of 127 mA/m^2 (Fig. 6).

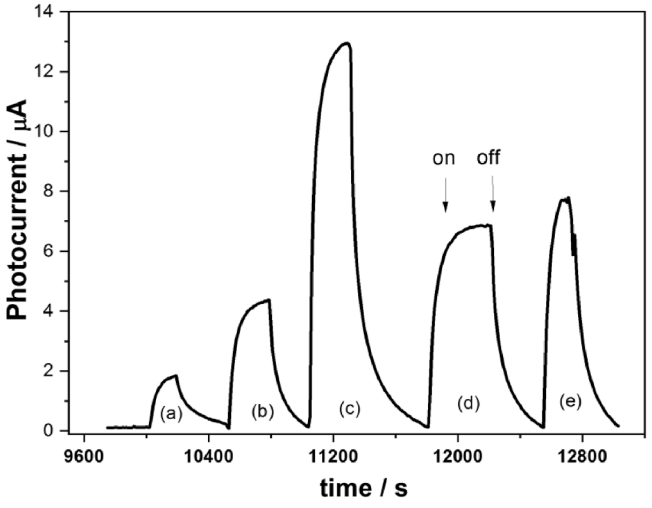

Fig. 3. Photocurrent values obtained as a result of the cycle numbers of a) 20, b) 40, c) 60, d) 80, e)100, which must be applied to coat the gold electrode with P(DTP-Ph-NH_2) polymer film.

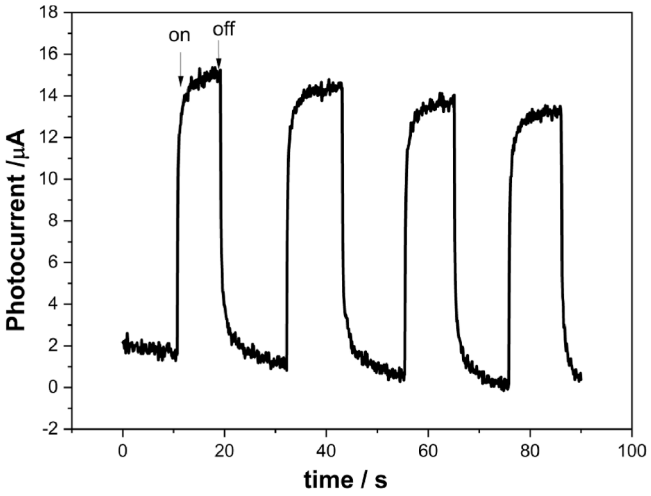

Fig. 4. Chronoamperometric on–off study showing that the oxygen gas of BPV is removed from the environment with the help of bilirubin oxidase enzyme.

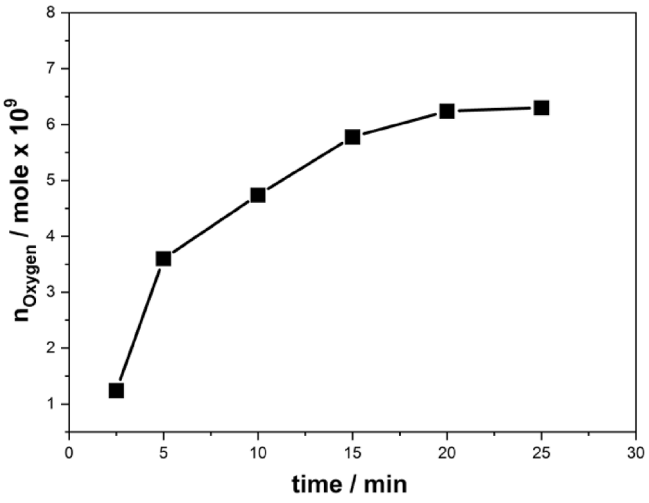

Fig. 5. Time-dependent oxygen gas generation of BPV system as a result of illumination for 2.5, 5, 10, 15, 20 and 25 min under the visible region light with a power of 1400 W/m^2.

3.3.3. H_2 gas generation in BPV cell

Figurative representation of hydrogen generation in a BPV solar cell was shown in Fig. 7 **(a)** Light with an intensity of 1400 W/m^2 was sent to the BPV system from the solar simulator and illuminated for periods of 2.5, 5, 7.5, 10, 12.5, 15 and 20 min. The H_2 gas generation by the BPV solar cell was obtained by analyzing a 1 mL (cm^3) gas sample taken from the system with the help of an injector by gas chromatography. In the calculations, after the system was illuminated with a light of 1400 W/m^2 for 20 min, 2.65 ± 0.75 × 10^{-8} mol/cm^3 H_2 gas was produced in the system (Fig. 7 **(b)**). In addition, the quantum efficiency for hydrogen gas generation was calculated as 5.5 percent. This study was repeated 3 times and reproducibility was observed in the results.

The H_2 gas generation in the BPV solar cell was found by analyzing a 1 mL (cm^3) gas retrieved from the system with the help of an injector by gas chromatography. The performance of the photoelectrochemical

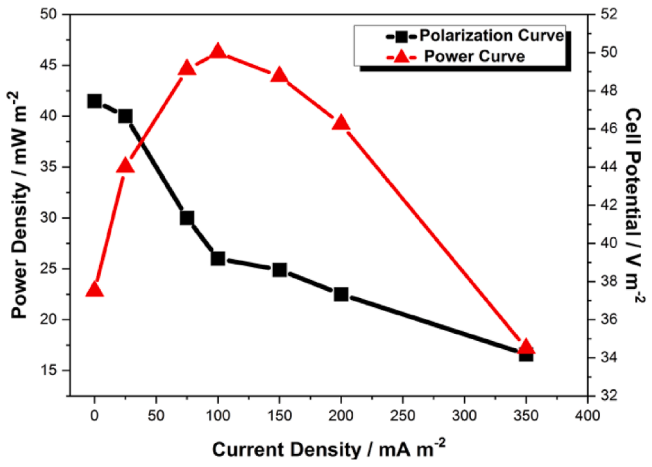

Fig. 6. Polarization and power curves of BPV obtained in 0.1 M pH 7.4 phosphate buffer solution under light and in an external resistance medium ranging from 100 Ω to 10 kΩ.

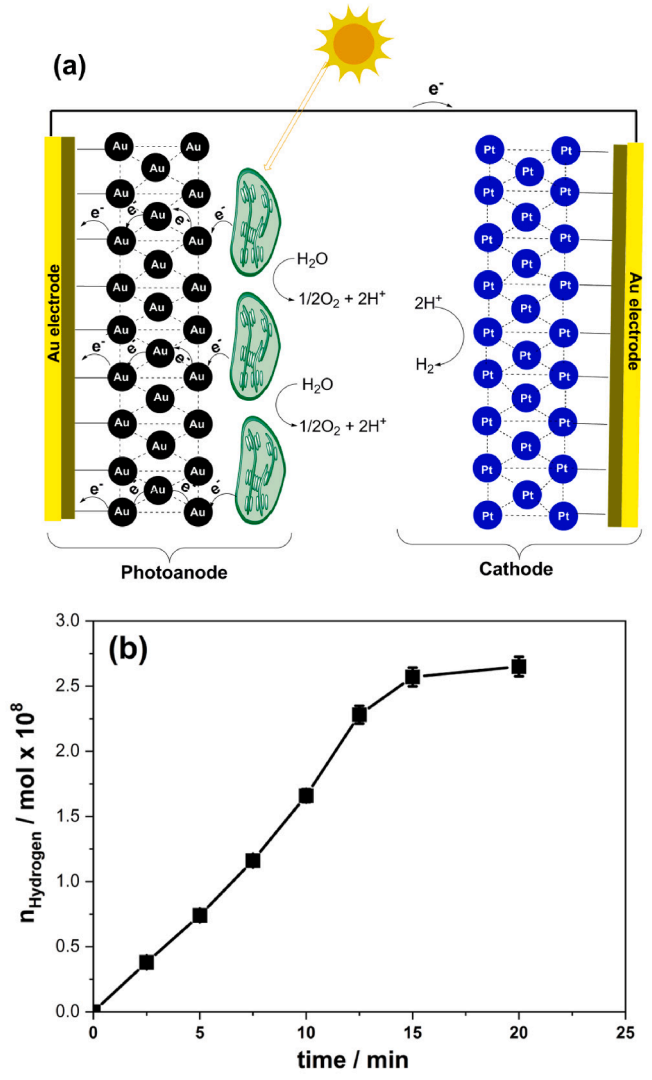

Fig. 7. (a) Figurative representation of hydrogen generation in a BPV solar cell (b) time dependent hydrogen gas generation of BPV solar cell.

solar cell, which produces photocurrent and hydrogen by decomposing water under visible light, is given in Table 1 together with similar studies in the literature [39,51–54]. In the comparison made according to H_2 gas generation, the cyanobacteria-based BPV system showed a very good performance with a generation of 265 μmol/L. This result reveals a comparable result with other reported studies. It is clearly seen that the obtained photocatalytic fuel cell produces both photocurrent and H_2 gas with high efficiency.

Oxygenated photosynthetic organisms convert the solar energy of water and CO_2 into O_2 and glucose. These cells also use a respiratory system functionally overlapping with the photosynthetic apparatus in order to metabolize sugars [46]. PS I in chlorophyll is responsible for this situation, since it is related to the oxidation of carbon materials in the respiratory systems of cyanobacteria and occurs in cases where there is no photosynthesis. It is aimed to produce photocurrent and hydrogen from respiration by transferring the electrons and protons here to the anode. For example, cyanobacteria oxidize glucose to acetyl coenzyme A (acetyl CoA) in their internal glycolytic process. In order to do this, it is necessary to prevent the photosynthesis of cyanobacteria in BPVs, that is, to block PS II. This was achieved by adding diuron to the environment of the anode to inhibit PS II of the cyanobacteria. When chemicals belonging to the diuron pesticide class were added to BPV cell, a decrease in the amount of photocurrent that would occur in the photovoltaic cell was observed due to the ability of this substance to block PSII in cyanobacteria and therefore inhibit photosynthesis. When the concentration of this substance was increased, the photocurrent produced in this BPV cell continued to decrease and no photocurrent formation was observed after a certain time. The representation of the photocurrents produced by the cyanobacteria-based biological photovoltaic cell by oxidation of water as a result of photosynthesis in the presence of 0, 0.2, 0.4, 0.8 and 1.5 mM diuron pesticide in water was shown in Fig. 8 **(a)**.

Then, in the presence of 1.6 mM diuron, which will completely block photosynthesis, when the BPV is illuminated with a light of visible light, a photocurrent of 30nA was obtained due to the rapid transfer of protons and electrons from PS I, which is actively working in the respiratory system of the cyanobacteria to the anode electrode. Then, when the concentration of glucose increase to be 2, 4, 6 and 8 mM in the medium in the presence of 1.6 mM diuron, the photocurrent obtained by increasing the amount of electrons transferred by PSI due to the cyanobacteria oxidizing and degrading the glucose by the respiratory system is obtained in the presence of 6 mM glucose. It went up to 0.7 μA. When the amount of glucose in the medium was increased to 8 mM, the photocurrent value decreased and 6 mM was found as the optimum glucose concentration (Fig. 8 **(b))**. In order to understand that the photocurrent produced in the presence of diuron and glucose is really produced by the respiratory (respiratory) system of the cyanobacteria, iodoacetate, which blocks the respiratory (respiratory) system of the cyanobacteria, was used. When iodoacetate with 0.2, 0.4, 0.8, 1.5 and 2.5 mM concentration values was added to the BPV solar cell illuminated with 1400 W/m^2 light in the presence of 1.6 mM diuron and 6 mM glucose, it was observed that the photocurrent produced by the respiratory (respirator) system of the cyanobacteria was seriously reduced. The result observed as a result of this experiment proved that the general electron donor for the formation of photocurrent is the respiratory

Table 1
Comparison of photocatalytic water separation performance based on H_2 gas generation.

Material	Light Source	H_2 gas concentration	Reference
Calyx/Cyanine/IrO_2	visible region light	125 μmol/L	[39]
FTO/SnO_2/TiO_2	visible region light	45 μmol/L	[51]
p-$LaFeO_3$/Fe_2O_3	visible region light	80 μmol/L	[52]
Co_3O_4 Quantum Dot	visible region light	0.79 μmol/L	[53]
Co_3O_4-TiO_2	visible region light	8.16 μmol/L	[54]
BPV	visible region light	265 μmol/L	This study

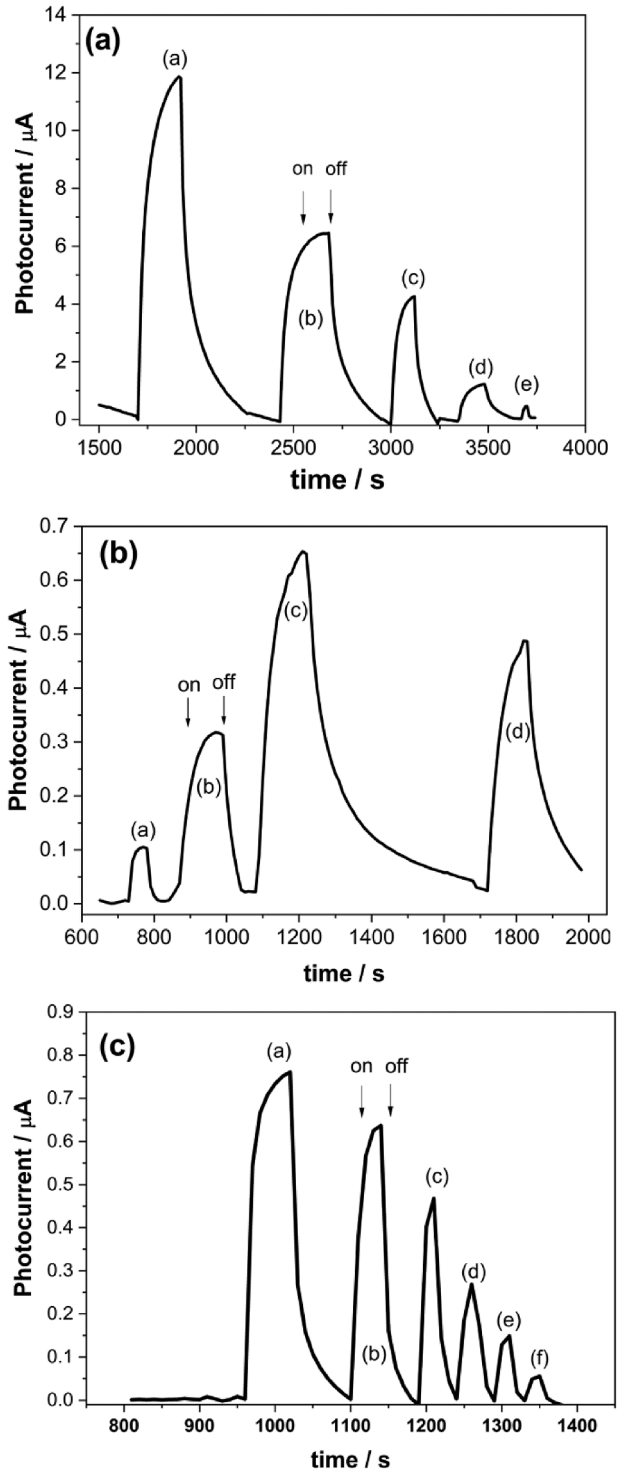

Fig. 8. (a) Chronoamperometric on–off study of photocurrents produced by BPV solar cell by oxidation of water as a result of photosynthesis in the presence of (a) 0, (b) 0.2, (c) 0.4, (d) 0.8 and (e) 1.5 mM diuron pesticide in water (in phosphate buffer (pH = 7.4) and under visible light at 1400 W/m^2 power) (b) Photocurrent values produced by the BPV solar cell in the presence of (a) 2 mM, (b) 4 mM, (c) 6 mM and (d) 8 mM glucose (all experiments were performed under a 0 V potential difference and a visible light of 1400 W/m^2 in the presence of 1.6 mM diuron) (c) BPV solar cell chronoamperometric on–off study in the presence of 1.6 M diuron, 6 mM glucose and (a) 0, (b) 0.2, (c) 0.4, (d) 0.8, (e) 1.5, (f) 2.5 mM iodoacetate ((in phosphate buffer solution (pH = 7.4) and under visible light with 1400 W/m^2 power).

(respirator) system (Fig. 8**(c)**) [46].

3.3.4. Power generation of the BPV by the respiratory (respirator) system

Power generation of the BPV by the respiratory (respirator) system, with the polarization curve using 100 Ω to 10 kΩ resistors connected in series with the BPV during measurements under 1400 W/m^2 visible light illumination in the presence of 1.6 mM diuron and 6 mM glucose. The power output was calculated from 1.25 to 4.3 mW/m^2 in the light environment. The maximum power generation of the BPV at pseudo steady state was reached as 4.50 mW/m^2 at a current density of 17 mA/m^2 (Fig. 9 **(a)**). In the presence of 1.6 mM diuron and 6 mM glucose, the BPV system was illuminated for 2.5, 5, 7.5, 10, 12.5, 15 and 20 min by sending light with an intensity of 1400 W/m^2 from the solar simulator. The H_2 gas formation produced by the BPV solar cell was obtained by analyzing a 1 mL (cm^3) gas sample taken with the help of an injector by gas chromatography. In the calculations, after the system was illuminated with a light of 1400 W/m^2 for 20 min, hydrogen gas of $4 \pm 0.35 \times 10^{-9}$ mol/cm^3 (4 μmol/L) was produced in the system (Fig. 9 **(b)**). In addition, the quantum efficiency for hydrogen gas generation was calculated as 1.75 %. This study was repeated 3 times and reproducibility was observed in the results.

4. Conclusions

In this project, BPV cells that can produce photocurrent and H_2 gas at the same time in an efficient, inexpensive, easy way by using both

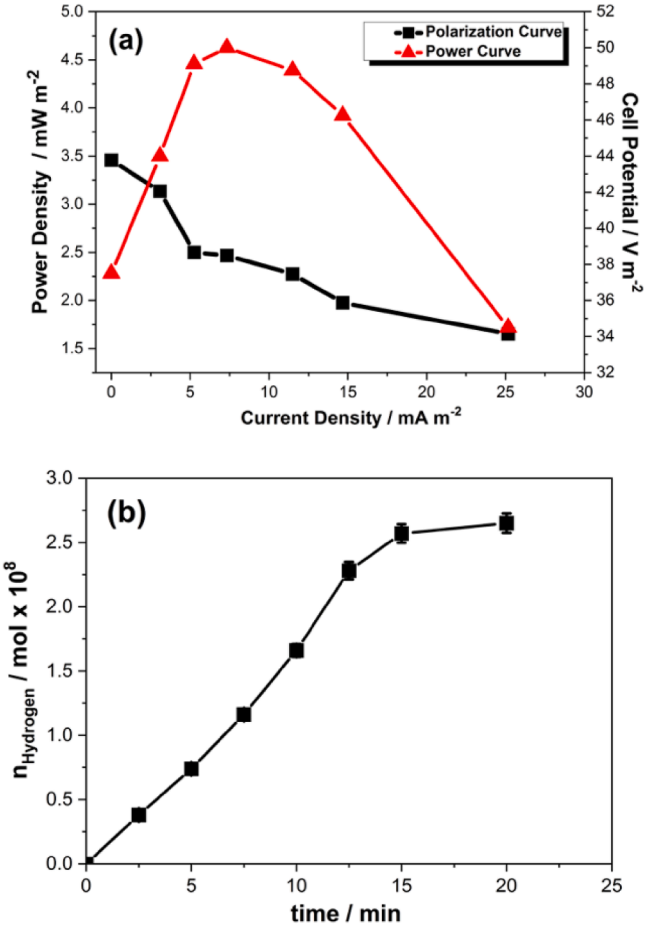

Fig. 9. (a) Polarization and power curves of BPV in 0.1 M pH 7.4 phosphate buffer solution in the presence of 1.6 mM diuron and 6 mM glucose under visible light illumination of 1400 W/m^2 and external resistance ranging from 100 Ω to 10 kΩ (b) Time-dependent hydrogen gas generation through the respiratory (respirator) system of cyanobacteria in the BPV solar cell.

photosynthesis and respiration properties of cyanobacteria under constant potential and visible region light were made using cyanobacteria (Leptolyngbia sp.). The photoanode, by coating the cyanobacteria on the structure that will be formed as a result of electrochemical polymerization of aniline-modified Au NPs to Au electrode coated with amine-functional DTP conductive polymer (P(DTP-Ph-NH_2)) with conductive oligoaniline bonds and the photoanode with aniline-functional SNS conductive polymer modified Au electrode acted as the cathode. When the system was operated under a constant potential by illuminating the visible region with light, the water was decomposed by oxidation through photosynthesis by cyanobacteria and the BPV solar cell system. At the same time, photocurrent produced oxygen (on the anode side of the system), hydrogen gas (electrochemical reduction of protons on the cathode side by Pt NPs. However, photosynthesis was inhibited by adding a PS II inhibitor called diuron to the medium. Then, when the system is illuminated under constant potential in the glucose medium by adding glucose to the medium, it was observed that the glucose was oxidized by taking advantage of the respiratory system possessed by cyanobacteria, and the electrons to be formed in PS I were transported to the anode and protons to the cathode and reduced. With this event, it has been revealed that photocurrent and hydrogen gas occur at the same time. Thus, hydrogen and photocurrent were obtained by taking advantage of both photosynthesis and respiratory (respiratory) system properties of cyanobacteria. As a result of electropolymerization of pyrrole-functional Au NPs on a Au electrode coated with amine-modified DTP polymer, the transfer of electrons to the electrode has been observed to occur rapidly. In addition, it was understood that the conductivity of the P(DTP-Ph-NH_2) polymer and Au NPs further increased the rate of this electron transfer. Thus, in both methods (photosynthesis and respiratory system), high amount of photocurrent and hydrogen were obtained as a result of very fast electron transfer.

CRediT authorship contribution statement

Buket Bezgin Carbas: Writing – original draft, Methodology, Investigation. **Menşure Güler:** Data curation, Investigation, Methodology. **Kamile Yücel:** Data curation, Formal analysis, Investigation. **Huseyin Bekir Yildiz:** Writing – review & editing, Conceptualization, Formal analysis, Investigation, Supervision.

Declaration of Competing Interest

The authors declare that they have no known competing financial interests or personal relationships that could have appeared to influence the work reported in this paper.

Data availability

The authors do not have permission to share data.

Acknowledgements

This study was supported by TUBITAK 2209-B Undergraduate Research Projects Support Program for Industry (Project Application Number:1139B412000335). We also thank TEKNOFEST 2021 Biotechnology Innovation Competition.

Appendix A. Supplementary data

Supplementary data to this article can be found online at https://doi.org/10.1016/j.jphotochem.2023.114764.

References

[1] R.A. Bullen, T.C. Arnot, J.B. Lakeman, F.C. Walsh, Biofuel cells and their development, Biosens. Bioelectron. 21 (2006) 2015–2045. https://doi.org/10.1016/j.bios.2006.01.030.
[2] B.E. Logan, B. Hamelers, R. Rozendal, U. Schröder, J. Keller, S. Freguia, P. Aelterman, W. Verstraete, K. Rabaey, Microbial Fuel Cells: Methodology and Technology, Environ. Sci. Tech. 40 (2006) 5181–5192, https://doi.org/10.1021/es0605016.
[3] N. Rashid, Y.-F. Cui, M. Saif Ur Rehman, J.-I. Han, Enhanced electricity generation by using algae biomass and activated sludge in microbial fuel cell, Sci. Total Environ. 456–457 (2013) 91–94. https://doi.org/10.1016/j.scitotenv.2013.03.067.
[4] M. Sawa, A. Fantuzzi, P. Bombelli, C.J. Howe, K. Hellgardt, P.J. Nixon, Electricity generation from digitally printed cyanobacteria, Nat. Commun. 8 (2017) 1327, https://doi.org/10.1038/s41467-017-01084-4.
[5] D.P.B.T.B. Strik, H.V.M. Hamelers (Bert), J.F.H. Snel, C.J.N. Buisman, Green electricity production with living plants and bacteria in a fuel cell, Int. J. Energy Res. 32 (9) (2008) 870–876.
[6] H.H. W., The use of energy from sunlight by photosynthesis is the basis of life on earth, Plant Biochem. (2005) 52–56. https://cir.nii.ac.jp/crid/1570009751310928640.
[7] Y. Zou, J. Pisciotta, R.B. Billmyre, I.V. Baskakov, Photosynthetic microbial fuel cells with positive light response, Biotechnol. Bioeng. 104 (2009) 939–946, https://doi.org/10.1002/bit.22466.
[8] A.J. McCormick, P. Bombelli, A.M. Scott, A.J. Philips, A.G. Smith, A.C. Fisher, C. J. Howe, Photosynthetic biofilms in pure culture harness solar energy in a mediatorless bio-photovoltaic cell (BPV) system, Energ. Environ. Sci. 4 (2011) 4699–4709, https://doi.org/10.1039/C1EE01965A.
[9] Y. Zhang, J.S. Noori, I. Angelidaki, Simultaneous organic carbon, nutrients removal and energy production in a photomicrobial fuel cell (PFC), Energ. Environ. Sci. 4 (2011) 4340–4346, https://doi.org/10.1039/C1EE02089G.
[10] M. Rosenbaum, U. Schröder, Photomicrobial Solar and Fuel Cells, Electroanalysis 22 (2010) 844–855. https://doi.org/10.1002/elan.200800005.
[11] K.P. Sokol, D. Mersch, V. Hartmann, J.Z. Zhang, M.M. Nowaczyk, M. Rögner, A. Ruff, W. Schuhmann, N. Plumeré, E. Reisner, Rational wiring of photosystem II to hierarchical indium tin oxide electrodes using redox polymers, Energ. Environ. Sci. 9 (12) (2016) 3698–3709, https://doi.org/10.1039/C6EE01363E.
[12] A. Badura, T. Kothe, W. Schuhmann, M. Rögner, Wiring photosynthetic enzymes to electrodes, Energ. Environ. Sci. 4 (2011) 3263–3274, https://doi.org/10.1039/C1EE01285A.
[13] P.N. Ciesielski, C.J. Faulkner, M.T. Irwin, J.M. Gregory, N.H. Tolk, D.E. Cliffel, G. K. Jennings, Enhanced Photocurrent Production by Photosystem I Multilayer Assemblies, Adv. Funct. Mater. 20 (2010) 4048–4054. https://doi.org/10.1002/adfm.201001193.
[14] L. Frolov, O. Wilner, C. Carmeli, I. Carmeli, Fabrication of Oriented Multilayers of Photosystem I Proteins on Solid Surfaces by Auto-Metallization, Adv. Mater. 20 (2008) 263–266. https://doi.org/10.1002/adma.200701474.
[15] G. LeBlanc, G. Chen, E.A. Gizzie, G.K. Jennings, D.E. Cliffel, Enhanced Photocurrents of Photosystem I Films on p-Doped Silicon, Adv. Mater. 24 (2012) 5959–5962. https://doi.org/10.1002/adma.201202794.
[16] O. Yehezkeli, O.I. Wilner, R. Tel-Vered, D. Roizman-Sade, R. Nechushtai, I. Willner, Generation of Photocurrents by Bis-aniline-Cross-Linked Pt Nanoparticle/Photosystem I Composites on Electrodes, J. Phys. Chem. B 114 (2010) 14383–14388, https://doi.org/10.1021/jp100454u.
[17] J.O. Calkins, Y. Umasankar, H. O'Neill, R.P. Ramasamy, High photo-electrochemical activity of thylakoid–carbon nanotube composites for photosynthetic energy conversion, Energ. Environ. Sci. 6 (2013) 1891–1900, https://doi.org/10.1039/C3EE40634B.
[18] N. Yang, Y. Zhang, J.E. Halpert, J. Zhai, D. Wang, L. Jiang, Granum-Like Stacking Structures with TiO2–Graphene Nanosheets for Improving Photo-electric Conversion, Small 8 (2012) 1762–1770. https://doi.org/10.1002/smll.201200079.
[19] K. Hasan, E. Çevik, E. Sperling, M.A. Packer, D. Leech, L. Gorton, Photoelectrochemical Wiring of Paulschulzia pseudovolvox (Algae) to Osmium Polymer Modified Electrodes for Harnessing Solar Energy, Adv. Energy Mater. 5 (22) (2015) 1501100. https://doi.org/10.1002/aenm.201501100.
[20] G. Pankratova, D. Pankratov, C. Di Bari, A. Goñi-Urtiaga, M.D. Toscano, Q. Chi, M. Pita, L. Gorton, A.L. De Lacey, Three-Dimensional Graphene Matrix-Supported and Thylakoid Membrane-Based High-Performance Bioelectrochemical Solar Cell, ACS Appl. Energy Mater. 1 (2018) 319–323, https://doi.org/10.1021/acsaem.7b00249.
[21] E. Cevik, B.B. Carbas, M. Senel, H.B. Yildiz, Construction of conducting polymer/cytochrome C/thylakoid membrane based photo-bioelectrochemical fuel cells generating high photocurrent via photosynthesis, Biosens. Bioelectron. 113 (2018) 25–31.
[22] K. Hasan, Y. Dilgin, S.C. Emek, M. Tavahodi, H.-E. Åkerlund, P.-Å. Albertsson, L. Gorton, Photoelectrochemical Communication between Thylakoid Membranes and Gold Electrodes through Different Quinone Derivatives, ChemElectroChem 1 (2014) 131–139. https://doi.org/10.1002/celc.201300148.
[23] F.-L. Ng, S.-M. Phang, V. Periasamy, K. Yunus, A.C. Fisher, N. Lebedev, Evaluation of Algal Biofilms on Indium Tin Oxide (ITO) for Use in Biophotovoltaic Platforms Based on Photosynthetic Performance, PLoS One 9 (5) (2014) e97643.
[24] Yildiz, H. B., Cevik, E., & Bezgin Carbas, B. (2019). Chapter 3 - Nanotechnology for biological photovoltaics; industrial applications of nanomaterials. In S. Thomas, Y. Grohens, & Y. B. B. T.-I. A. of N. Pottathara (Eds.), *Micro and Nano Technologies* (pp.

65–89). Elsevier. https://doi.org/https://doi.org/10.1016/B978-0-12-815749-7.00003-7.
[25] R.U. Tanvir, J. Zhang, T. Canter, D. Chen, J. Lu, Z. Hu, Harnessing solar energy using phototrophic microorganisms: A sustainable pathway to bioenergy, biomaterials, and environmental solutions, Renew. Sustain. Energy Rev. 146 (2021), 111181. https://doi.org/10.1016/j.rser.2021.111181.
[26] K. Nishio, K. Hashimoto, K. Watanabe, Light/electricity conversion by defined cocultures of Chlamydomonas and Geobacter, J. Biosci. Bioeng. 115 (2013) 412–417. https://doi.org/10.1016/j.jbiosc.2012.10.015.
[27] P. Bombelli, R.W. Bradley, A.M. Scott, A.J. Philips, A.J. McCormick, S.M. Cruz, A. Anderson, K. Yunus, D.S. Bendall, P.J. Cameron, J.M. Davies, A.G. Smith, C. J. Howe, A.C. Fisher, Quantitative analysis of the factors limiting solar power transduction by Synechocystis sp. PCC 6803 in biological photovoltaic devices, Energ. Environ. Sci. 4 (2011) 4690–4698, https://doi.org/10.1039/C1EE02531G.
[28] M. Torimura, A. Miki, A. Wadano, K. Kano, T. Ikeda, Electrochemical investigation of cyanobacteria Synechococcus sp. PCC7942-catalyzed photoreduction of exogenous quinones and photoelectrochemical oxidation of water, J. Electroanal. Chem. 496 (2001) 21–28. https://doi.org/10.1016/S0022-0728(00)00253-9.
[29] Y.A. Gorby, S. Yanina, J.S. McLean, K.M. Rosso, D. Moyles, A. Dohnalkova, T. J. Beveridge, I.S. Chang, B.H. Kim, K.S. Kim, D.E. Culley, S.B. Reed, M.F. Romine, D.A. Saffarini, E.A. Hill, L. Shi, D.A. Elias, D.W. Kennedy, G. Pinchuk, K. Watanabe, S. Ishii, B. Logan, K.H. Nealson, J.K. Fredrickson, Electrically conductive bacterial nanowires produced by Shewanella oneidensis strain MR-1 and other microorganisms, Proc. Natl. Acad. Sci. U.S.A. 103 (30) (2006) 11358–11363.
[30] E. Cevik, M. Buyukharman, H.B. Yildiz, Construction of efficient bioelectrochemical devices: Improved electricity production from cyanobacteria (Leptolyngbia sp.) based on π-conjugated conducting polymer/gold nanoparticle composite interfaces, Biotechnol. Bioeng. 116 (2019) 757–768. https://doi.org/10.1002/bit.26885.
[31] K. Hasan, H. Bekir Yildiz, E. Sperling, P.Ó. Conghaile, M.A. Packer, D. Leech, C. Hägerhäll, L. Gorton, Photo-electrochemical communication between cyanobacteria (Leptolyngbia sp.) and osmium redox polymer modified electrodes, PCCP 16 (2014) 24676–24680, https://doi.org/10.1039/C4CP04307C.
[32] X. Chen, S. Shen, L. Guo, S.S. Mao, Semiconductor-based Photocatalytic Hydrogen Generation, Chem. Rev. 110 (2010) 6503–6570, https://doi.org/10.1021/cr1001645.
[33] C.-H. Liao, C.-W. Huang, J.C.S. Wu, Hydrogen Production from Semiconductor-based Photocatalysis via Water Splitting, Catalysts 2 (4) (2012) 490–516.
[34] Y. Chen, Y. Wang, H. Xu, G. Xiong, Efficient production of hydrogen from natural gas steam reforming in palladium membrane reactor, Appl. Catal. B 81 (2008) 283–294. https://doi.org/10.1016/j.apcatb.2007.10.024.
[35] A. Damien, Hydrogène par électrolyse de l'eau, Techniques de l'ingénieur Vol, J6, N J. 6366 (1992) 12–1992.
[36] C. Gaudillere, L. Navarrete, J.M. Serra, Syngas production at intermediate temperature through H2O and CO2 electrolysis with a Cu-based solid oxide electrolyzer cell, Int. J. Hydrogen Energy 39 (2014) 3047–3054. https://doi.org/10.1016/j.ijhydene.2013.12.045.
[37] G.F. Naterer, I. Dincer, C. Zamfirescu (Eds.), Hydrogen Production from Nuclear Energy, Springer London, London, 2013.
[38] S. Turn, C. Kinoshita, Z. Zhang, D. Ishimura, J. Zhou, An experimental investigation of hydrogen production from biomass gasification, Int. J. Hydrogen Energy 23 (1998) 641–648. https://doi.org/10.1016/S0360-3199(97)00118-3.
[39] M. Tekin, E. Cevik, S. Sayin, H.B. Yildiz, Photocurrent and hydrogen production by overall water splitting based on polymeric composite Calix[n]arene/Cyanin Dye/IrO2 nanoparticle, Int. J. Hydrogen Energy 45 (2020) 19869–19879. https://doi.org/10.1016/j.ijhydene.2020.05.126.
[40] H.B. Yildiz, B.B. Carbas, S. Sonmezoglu, M. Karaman, L. Toppare, A photoelectrochemical device for water splitting using oligoaniline-crosslinked [Ru(bpy)2(bpyCONHArNH2)]+2 dye/IrO2 nanoparticle array on TiO2 photonic crystal modified electrode, Int. J. Hydrogen Energy 41 (2016) 14615–14629. https://doi.org/10.1016/j.ijhydene.2016.04.249.
[41] B.E. Logan, D. Call, S. Cheng, H.V.M. Hamelers, T.H.J.A. Sleutels, A.W. Jeremiasse, R.A. Rozendal, Microbial Electrolysis Cells for High Yield Hydrogen Gas Production from Organic Matter, Environ. Sci. Tech. 42 (2008) 8630–8640, https://doi.org/10.1021/es801553z.
[42] D.K. Bora, A. Braun, E.C. Constable, "In rust we trust". Hematite – the prospective inorganic backbone for artificial photosynthesis, Energ. Environ. Sci. 6 (2013) 407–425, https://doi.org/10.1039/C2EE23668K.
[43] C. Herrero, A. Quaranta, W. Leibl, A.W. Rutherford, A. Aukauloo, Artificial photosynthetic systems. Using light and water to provide electrons and protons for the synthesis of a fuel, Energy Environ. Sci. 4 (2011) 2353–2365, https://doi.org/10.1039/C0EE00645A.
[44] B. Min, S. Cheng, B.E. Logan, Electricity generation using membrane and salt bridge microbial fuel cells, Water Res. 39 (2005) 1675–1686. https://doi.org/10.1016/j.watres.2005.02.002.
[45] A.J. McCormick, P. Bombelli, D.J. Lea-Smith, R.W. Bradley, A.M. Scott, A.C. Fisher, A.G. Smith, C.J. Howe, Hydrogen production through oxygenic photosynthesis using the cyanobacterium Synechocystis sp. PCC 6803 in a bio-photoelectrolysis cell (BPE) system, Energ. Environ. Sci. 6 (2013) 2682–2690, https://doi.org/10.1039/C3EE40491A.
[46] G. Saper, D. Kallmann, F. Conzuelo, F. Zhao, T.N. Tóth, V. Liveanu, S. Meir, J. Szymanski, A. Aharoni, W. Schuhmann, A. Rothschild, G. Schuster, N. Adir, Live cyanobacteria produce photocurrent and hydrogen using both the respiratory and photosynthetic systems, Nat. Commun. 9 (2018) 2168, https://doi.org/10.1038/s41467-018-04613-x.
[47] E. Yildiz, P. Camurlu, C. Tanyeli, I. Akhmedov, L. Toppare, A soluble conducting polymer of 4-(2,5-di(thiophen-2-yl)-1H-pyrrol-1-yl)benzenamine and its multichromic copolymer with EDOT, J. Electroanal. Chem. 612 (2008) 247–256. https://doi.org/10.1016/j.jelechem.2007.10.004.
[48] Y.A. Udum, H.B. Yıldız, H. Azak, E. Sahin, O. Talaz, A. Çırpan, L. Toppare, Synthesis and spectroelectrochemistry of dithieno(3,2-b:2′,3′-d)pyrrole derivatives, Journal of Applied Polymer Science. 131 (2014). https://doi.org/https://doi.org/10.1002/app.40701.
[49] H.B. Yildiz, R. Tel-Vered, I. Willner, Solar Cells with Enhanced Photocurrent Efficiencies Using Oligoaniline-Crosslinked Au/CdS Nanoparticles Arrays on Electrodes, Adv. Funct. Mater. 18 (2008) 3497–3505. https://doi.org/10.1002/adfm.200800810.
[50] R. Tel-Vered, H.B. Yildiz, Y.-M. Yan, I. Willner, Plugging into Enzymes with Light: Photonic "Wiring" of Enzymes with Electrodes for Photobiofuel Cells, Small 6 (2010) 1593–1597. https://doi.org/10.1002/smll.201000296.
[51] L. Alibabaei, B.D. Sherman, M.R. Norris, M.K. Brennaman, T.J. Meyer, Visible photoelectrochemical water splitting into H2 and O2 in a dye-sensitized photoelectrosynthesis cell, Proc. Natl. Acad. Sci. 112 (2015) 5899–5902, https://doi.org/10.1073/pnas.1506111112.
[52] Q. Yu, X. Meng, T. Wang, P. Li, L. Liu, K. Chang, G. Liu, J. Ye, A highly durable p-LaFeO3/n-Fe2O3 photocell for effective water splitting under visible light, Chem. Commun. 51 (2015) 3630–3633, https://doi.org/10.1039/C4CC09240F.
[53] N. Shi, W. Cheng, H. Zhou, T. Fan, M. Niederberger, Facile synthesis of monodisperse Co3O4 quantum dots with efficient oxygen evolution activity, Chem. Commun. 51 (2015) 1338–1340, https://doi.org/10.1039/C4CC08179J.
[54] Q. Zhang, Z. Hai, A. Jian, H. Xu, C. Xue, S. Sang, Synthesis of p-Co3O4/n-TiO2 Nanoparticles for Overall Water Splitting under Visible Light Irradiation, Nanomaterials 6 (8) (2016) 138.